Supporting Information

Guo et al. 10.1073/pnas.1008946107

SI Materials and Methods

***Caenorhabditis elegans* Strains.** Strains of *C. elegans* were cultured at 20 °C by using standard procedures (1). The N2 Bristol strain was used as the wild-type strain. Mutations used are described in *C. elegans II* (2), unless otherwise indicated. Linkage group I (LGI): *unc-108(n3263)* (3), *dpy-5(e61)*, *unc-75(e950)*; LGII: *bli-2 (e768)*, *unc-4(e120)*; LGIII: *dpy-1(e1)*, *unc-45(e286)*; LGIV: *ced-3(n717)*, *dpy-13(e184sd)*, *unc-8(n491sd)*; LGV: *lon-3(e2175)*, *unc-76(e911)*; LGX: *lon-2(e678)*, *unc-27(e155)*, *unc-3(e151)*, *rab-14(qx18)* and *rab-14(tm2095)* (this study), *lin-15(n765ts)*.

opIs334 ($P_{ced\text{-}1}$YFP::2xFYVE, a gift of K. S. Ravichandran, University of Virginia, Charlottesville, VA, and M. O. Hengartner, University of Zurich, Zurich, Switzerland). *kxEx152* ($P_{asm\text{-}1}$*asm-1::mcherry*, a gift of Greg Hermann, Lewis and Clark College, Portland, OR).

Other strains used in this study carrying integrated or transgenic arrays are as follows: *qxIs65* ($P_{ced\text{-}1}$*gfp::rab-5*), *qxIs66* ($P_{ced\text{-}1}$*gfp::rab-7*), *qxIs86* ($P_{rab\text{-}14}$*gfp::rab-14*), *qxIs105* ($P_{rab\text{-}14}$*mcherry::rab-14*), *qxIs132* [$P_{rab\text{-}14}$*gfp::rab-14*(T67M)], *qxIs133* [P_{hsp}*rab-14*(T67M)], *qxIs146* [$P_{ced\text{-}1}$GFP::2xFYVE], *qxIs163* [$P_{rab\text{-}14}$*gfp::rab-14*(S25N)], *qxIs234* ($P_{ced\text{-}1}$*gfp::unc-108*), *qxIs281* ($P_{ced\text{-}1}$*ctns-1::gfp*), *qxEx600* ($P_{rab\text{-}14}$*gfp::rab-14*), *qxEx1285* [$P_{rab\text{-}14}$*gfp::rab-14*(Q70L)] *qxEx2482* ($P_{ced\text{-}1}$*nuc-1::mcherry*), *qxEx2467* ($P_{ced\text{-}1}$*cpr-6::mcherry*), *qxEx3272* (P_{hsp}*rab-14*), *qxEx1469* [P_{hsp}*rab-14*(S25N)], *qxEx942* [P_{hsp}*rab-14* (Q70L)], *qxEx2900* ($P_{ced\text{-}1}$*gfp::rab-5*), *qxEx2712* ($P_{ced\text{-}1}$*nuc-1::mcherry* + $P_{ced\text{-}1}$*ctns-1::gfp*), *qxEx2994* ($P_{ced\text{-}1}$*cpr-6::mcherry* + $P_{ced\text{-}1}$*ctns-1::gfp*), *qxEx2995* ($P_{ced\text{-}1}$*nuc-1::mcherry* + P_{hsp}*gfp::rab-14*), *qxEx2783* ($P_{ced\text{-}1}$*nuc-1::mcherry* + $P_{ced\text{-}1}$*gfp::unc-108*), *qxEx2939* ($P_{ced\text{-}1}$mCHERRY::FAPP1-PH + P_{hsp}*gfp::rab-14*), *qxEx2953* ($P_{ced\text{-}1}$mCHERRY::FAPP1-PH + $P_{ced\text{-}1}$*gfp::unc-108*), *qxEx2941* ($P_{ced\text{-}1}$*mcherry::rab-5* + P_{hsp}*gfp::rab-14*), *qxEx2961* ($P_{ced\text{-}1}$*mcherry::rab-5* + $P_{ced\text{-}1}$*gfp::unc-108*).

Molecular Cloning of *rab-14*. Standard ethylmethane sulphonate mutagenesis was performed on *sem-4(n1378);ttr-52(sm211)* hermaphrodites and candidate mutants were selected as described before with minor modifications (4, 5). Briefly, F1 adults that bag F2 mutant progeny, which contain many cell corpses at the L1 larval stage were rescued. Homozygous mutants were recovered by selecting animals whose progeny all contain persistent cell corpses at the L1 larval stage. *qx18* was isolated from such a screen and was backcrossed with N2 five times before further analysis.

qx18 was mapped to the right arm of chromosome X by using *lon-2 unc-27*. One more round of three point-mapping was performed by using *unc-3* (+21.27) *lin-15* (+22.95), which mapped *qx18* very close to the left side of *lin-15*. Transformation rescue experiments were then performed and one fosmid clone in this region, WRM0623Ca04, rescued the persistent cell corpse phenotype of the *qx18* mutant. Long PCR fragments covering different ORFs within the fosmid were amplified and tested for rescue activity and only one fragment covering K09A9.2 possessed rescue activity, which corresponds to the *rab-14* gene. The molecular lesion in *qx18* mutants was determined by sequencing the *rab-14* locus.

Quantification of Cell Corpse Appearance, Cell Death Events, Cell Corpse Duration, and Phagosome Maturation. The number of somatic cell corpses in the head region of living embryos and the number of germ cell corpses in one gonad arm at various adult ages were scored as described (6, 7). Four-dimensional (4D) microscopy analysis of cell corpse duration was performed at 20–22 °C as described before (8). To monitor the occurrence of embryonic cell death, embryos at the two-cell stage were mounted on agar pads and images in 40 *z* sections (0.5 μm per section) were captured every 1 min for 8 h by using a Zeiss Axioimager M1 microscope (Carl Zeiss). Images were processed and viewed using Axiovision Rel 4.7 software (Carl Zeiss). To quantify the percentage of germ cell corpses labeled by various phagosomal markers, adult animals (24 h after L4/adult molt) were dissected in gonad dissection buffer (60 mM NaCl, 32 mM KCl, 3 mM Na_2HPO_4, 2 mM $MgCl_2$, 20 mM Hepes, 50 μg/mL penicillin, 50 μg/mL streptomycin, 100 μg/mL neomycin, 10 mM Glucose, 33% FCS, and 2 mM $CaCl_2$) to expose their anterior gonads as described before examination by fluorescent microscopy (9). Time lapse imaging was performed by mounting adult animals (24 h after L4/adult molt) or embryos at the precomma or comma stage on agar pads in M9 buffer with 5 mM levamisole and images in 22-25 z series (1.0 μm/section) were captured every 1.5–2 min for 120 min using a Zeiss LSM 5 Pascal inverted confocal microscope with 488, 543, 514, and 458 lasers. Images were processed and viewed using LSM Image Browser software (Carl Zeiss).

Lysosensor, Lysotracker, and Hoechst 33342 Staining. Lysosensor, Lysotracker, or Hoechst 33342 staining was performed as described with some modifications (3). Briefly, adult animals (24 h after L4/adult molt) were dissected in gonad dissection buffer with 1 μM Lysosensor Green DND-189 or 10 μM Lysotracker Blue DND-22 or 1 μM Hoechst33342 (Invitrogen) and examined by fluorescent microscopy.

RNA Interference (RNAi). The bacterial feeding protocol was used in RNAi experiments as described (10). For *rab-14*, *gla-3*, *vps-34,* and *rab-7* RNAi, L4 larvae were treated with *rab-14* (pPD129.36-*rab-14*), *gla-3* (I-4C17), *vps-34* (pPD129.36-*vps-34*), or *rab-7* RNAi (II-8G13), and embryonic cell corpses were scored in the F1 generation. To quantify the number of germ cell copses, F1 L4 larvae were transferred to fresh RNAi plates and aged for 24 h before examination. For *rab-5* RNAi (I-4J01), L2 or L3 larvae were mounted on RNAi plates and germ cell corpses were scored 36 h after L4/adult molt.

Heat-Shock Experiments. To score the number of cell corpses at embryonic stages, young adults were moved to fresh NGM plates and cultured at 20 °C for 12 h, then incubated at 33 °C for 1 h, followed by recovery at 20 °C for 1.5 h. Adult worms were removed and embryos were incubated at 20 °C and scored for the number of cell corpses 5–10 h after treatment. To score the number of germ cell corpses, L4 larvae were moved to fresh NGM plates and heat-shocked at 33 °C every 12 h. The number of germ corpses was scored 48 h later.

Antibody Generation and Western Blot Analysis. The RAB-14 protein tagged with six Histidine residues (RAB-14-His_6) was expressed and purified from *E. coli* and used to raise rat polyclonal antibody against RAB-14. RAB-14 antibody was further purified by incubating 5 mL of rat serum with nitrocellulose membrane strips containing 2 mg of RAB-14-His_6 protein. Bound antibodies were eluted with 100 mM glycine-HCl (pH 2.5). For Western blot analysis, worm lysate obtained from 200 adult worms of indicated strains was resolved by SDS polyacrylamide gel and detected with purified anti-RAB-14 antibody. Immunofluorescence staining of RAB-14 in *C. elegans* embryos and sheath cells were also performed. Unfortunately, although a specific protein band with expected molecular weight of RAB-14 was revealed by Western blot analysis in wild-type but not *rab-14(tm2095)* mutant lysate, we

failed to detect specific staining patterns of RAB-14 in a whole-mount immunostaining assay with the same antibody.

Plasmid Construction. The sequences of the PCR primers mentioned in this section are presented in Table S1. To generate P_{rab-14}*gfp::rab-14*, a 1,334-bp *rab-14* genomic fragment was amplified by using primers PTJH54/PPFG60 and cloned into pPD49.26-*gfp*1 through its KpnI site. The resulting pPD49.26-*gfp::rab-14* was then ligated with the 2.1-kb promoter region of *rab-14* amplified by using primers PTJH48/PTJH53 through SphI and BamHI sites. A similar strategy was used to construct P_{rab-14}*mcherry::rab-14*, in which pPD49.26-*mcherry*1 was used instead of pPD49.26-*gfp*1. The S25N, T67M, and Q70L mutations were introduced into pPD49.26-*gfp::rab-14* by site-directed mutagenesis (QuikChange; Stratagene) using the primer pairs PPFG31/PPFG32 (S25N), PPFG53/PPFG54 (T67M), and PPFG33/PPFG34 (Q70L). To construct P_{hsp}*gfp::rab-14*, the genomic sequence of *gfp* without the stop codon was first cloned into pPD49.78 and pPD49.83 through NheI and KpnI sites. The resulting pPD49.78/pPD49.83-*gfp* was then ligated with the *rab-14* genomic fragment through the KpnI site. The wild-type or mutated *rab-14* genomic fragments (S25N, T67M, Q70L) were digested from P_{rab-14}*gfp::rab-14*(WT/S25N/T67M/Q70L) and cloned into pPD49.78 and pPD49.83 through the KpnI site to generate P_{hsp}*rab-14*(WT/S25N/T67M/Q70L). To get P_{rab-14}*rab-14*, a 3.4-kb genomic fragment of *rab-14* including a 2.1-kb promoter region was PCR-amplified by using primers PTJH48/PTJH49 and cloned into pPD49.26 through SphI and BamHI sites. To construct P_{ced-1}*rab-14* and P_{egl-1}*rab-14*, the full-length cDNA of *rab-14* was amplified from a *C. elegans* cDNA library (Invitrogen) and cloned into P_{ced-1} or P_{egl-1} vector through the NcoI or NheI/NcoI site, respectively. Mouse *Rab14* cDNA was amplified from a mouse brain cDNA library by using PPFG72/ PPFG71 and cloned into pPD49.78 and pPD49.83 to obtain P_{hsp}*mRab14*. To generate P_{ced-1}*nuc-1::mcherry* and P_{ced-1}*cpr-6::mcherry*, genomic fragments of *nuc-1* and *cpr-6* were amplified by using primers PPFG285/PPFG286 and PPFG271/PPFG272, respectively, and cloned into P_{ced-1}*mcherry*2 through XmaI and KpnI sites. To generate P_{ced-1}*mcherry::FAPP1-PH*, a cDNA fragment of the PH domain of human FAPP1 was amplified from 293T cells by using primers PPFG364/PPFG365 and cloned into P_{ced-1}*mcherry*1 through the KpnI site (11). To get P_{ced-1}*mcherry::rab-5*, the genomic fragment of *rab-5* was amplified by using primers PXCW241/PXCW243 and cloned into P_{ced-1}*mcherry*1 through the KpnI site.

1. Brenner S (1974) The genetics of Caenorhabditis elegans. *Genetics* 77:71–94.
2. Riddle DL, Blumenthal T, Meyer BJ, Priess JR (1997) *C. elegans II* (Cold Spring Harbor Lab Press, Plainview, NY).
3. Mangahas PM, Yu X, Miller KG, Zhou Z (2008) The small GTPase Rab2 functions in the removal of apoptotic cells in Caenorhabditis elegans. *J Cell Biol* 180:357–373.
4. Wang X, et al. (2010) Caenorhabditis elegans transthyretin-like protein TTR-52 mediates recognition of apoptotic cells by the CED-1 phagocyte receptor. *Nat Cell Biol* 9:541–549.
5. Ellis RE, Jacobson DM, Horvitz HR (1991) Genes required for the engulfment of cell corpses during programmed cell death in Caenorhabditis elegans. *Genetics* 129:79–94.
6. Gumienny TL, Lambie E, Hartwieg E, Horvitz HR, Hengartner MO (1999) Genetic control of programmed cell death in the Caenorhabditis elegans hermaphrodite germline. *Development* 126:1011–1022.
7. Wang X, Yang C, Chai J, Shi Y, Xue D (2002) Mechanisms of AIF-mediated apoptotic DNA degradation in Caenorhabditis elegans. *Science* 298:1587–1592.
8. Wang X, et al. (2003) Cell corpse engulfment mediated by C. elegans phosphatidylserine receptor through CED-5 and CED-12. *Science* 302:1563–1566.
9. Wang X, et al. (2007) C. elegans mitochondrial factor WAH-1 promotes phosphatidylserine externalization in apoptotic cells through phospholipid scramblase SCRM-1. *Nat Cell Biol* 9:541–549.
10. Kamath RS, Ahringer J (2003) Genome-wide RNAi screening in Caenorhabditis elegans. *Methods* 30:313–321.
11. Dippold HC, et al. (2009) GOLPH3 bridges phosphatidylinositol-4- phosphate and actomyosin to stretch and shape the Golgi to promote budding. *Cell* 139:337–351.

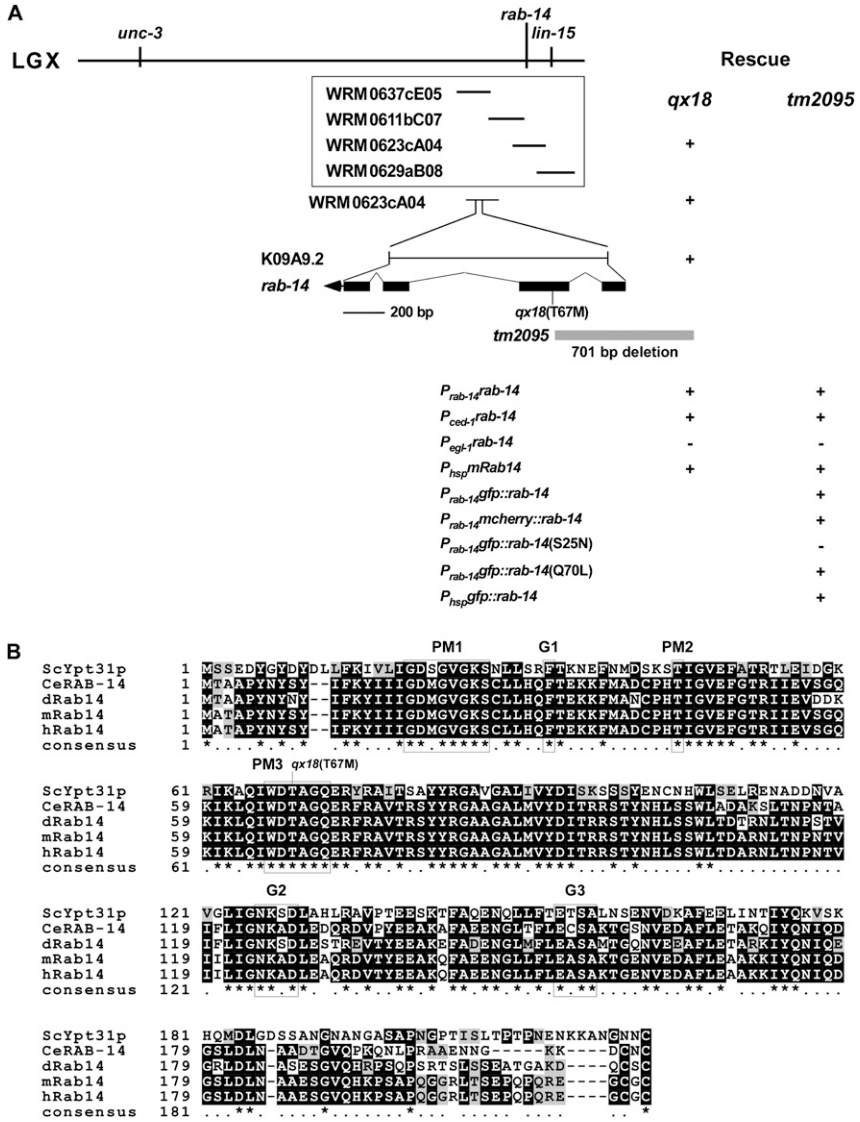

Fig. S1. Molecular cloning of *rab-14*. (*A*) The top bar indicates the genetic map of the *rab-14* region on the right arm of linkage group X, and the lower images show the rescue of *rab-14* mutants. Nontransgenic and transgenic embryos at the fourfold stage were scored for each construct. At least 15 animals (transgenic or nontransgenic) from each independent transgenic line were scored for at least three lines. The *rab-14* gene structure is shown with filled boxes representing exons and thin lines indicating introns. The arrow shows the direction of the *rab-14* transcript. The T67M mutation identified in the *qx18* mutant is marked, and the gray bar below the *rab-14* transcript delineates the 701-bp region of the *rab-14* gene removed in the deletion mutant *tm2095*. Constructs expressing GFP or mCHERRY fusions were also tested for their rescue activity in the germ line. (*B*) Sequence alignment of yeast Ypt31p, *C. elegans* RAB-14, and RAB14 from fly, mouse, and human. Identical residues are shaded in black and similar residues in gray. Residues that are identical in all five proteins are marked with an asterisk. PM1, 2, and 3 are motifs that bind the phosphate groups of GTP and the Mg^{2+} cofactor, whereas G1, 2, and 3 are motifs that contact the guanine base. The mutation identified in the *qx18* mutant is indicated.

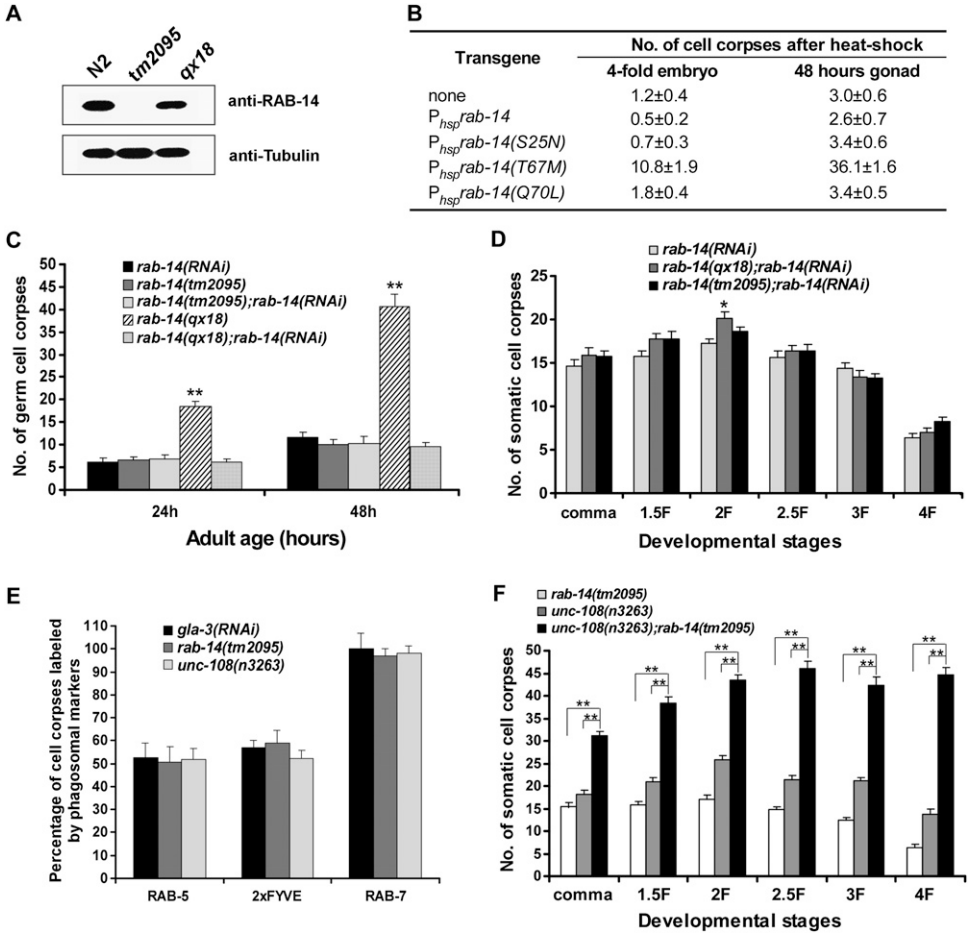

Fig. S2. *qx18* mutants show dominant negative effect in the clearance of germ cell corpses. (*A*) Western blot analysis of *rab-14* mutants. *C. elegans* lysates were made from adult wild-type (N2), *rab-14(tm2095)*, and *rab-14(qx18)* animals, and Western blot analysis was performed by using affinity-purified anti-RAB-14 antibodies. *C. elegans* Tublin was used as a loading control. (*B*) Overexpression of RAB-14(T67M) resulted in accumulation of cell corpses. The number of cell corpses in embryos at the fourfold stage or gonads from animals aged 48 h after L4/adult molt was scored in indicated strains. Data are shown as mean ± SEM. Heat-shock treatment was performed as described in *SI Materials and Methods*. (*C*) *rab-14(RNAi)* reduced the number of germ cell corpses in the *qx18* mutant. The number of germ cell corpses was scored and analyzed as described in Fig. 1. RNAi experiments were performed as described in *SI Materials and Methods*. (*D*) *rab-14(RNAi)* did not affect the number of somatic cell corpses in *qx18* or *tm2095* mutants. Cell corpses were scored and analyzed as descried in Fig. 1. (*E*) The percentage of germ cell corpses labeled by 2xFYVE, GFP::RAB-5, and GFP::RAB-7 was quantified in *gla-3(RNAi)*, *rab-14(tm2095),* or *unc-108(n3263)* animals. (*F*) Time-course analysis of cell corpse appearance during embryonic development was performed in *rab-14(tm2095)*, *unc-108(n3263)*, or *unc-108(n3263);rab-14 (tm2095)* mutants. In *B–F*, at least 15 animals were scored at each stage and error bars indicate SEM. In *C*, *D,* and *F*, data derived from different genetic backgrounds at multiple developmental stages were compared by two-way analysis of variance. Post hoc comparisons were carried out by using Fisher's PLSD (protected least squares difference). $*P < 0.05$; $**P < 0.0001$ and all other points had $P > 0.05$. In *E*, an unpaired *t* test was carried out by comparing all other datasets with that of *gla-3(RNAi)*.

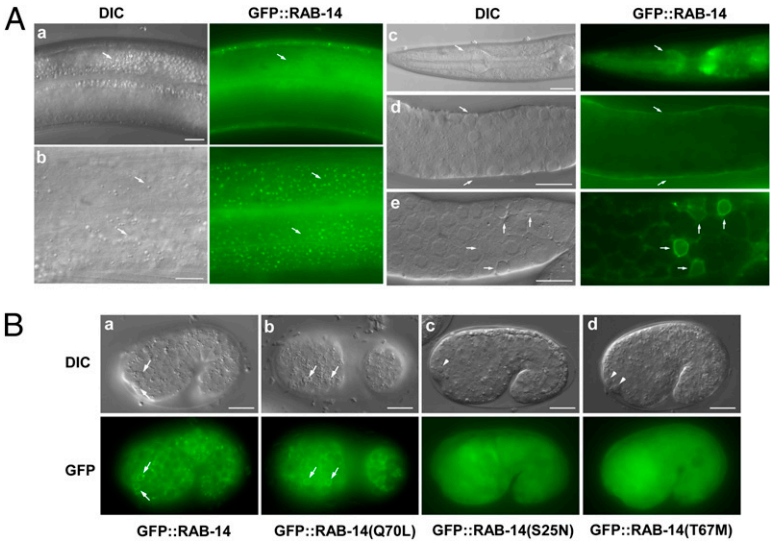

Fig. S3. *rab-14* is expressed in engulfing cells and clusters around cell corpses. (*A*) DIC and fluorescent images of wild-type animals expressing GFP::RAB-14 driven by the *rab-14* promoter (P_{rab-14}GFP::RAB-14). GFP::RAB-14 was observed in known engulfing cells including intestinal cells (*a*), hypodermal cells (*b*), pharyngeal muscle cells (*c*), and gonadal sheath cells (*d*). GFP::RAB-14 can be seen on the surface of germ cell corpses (*e*). Arrows point to different cell types and germ cell corpses labeled by GFP. (*B*) DIC and fluorescent images of wild-type embryos carrying GFP::RAB-14 (*a*), GFP::RAB-14(Q70L) (*b*), GFP::RAB-14(S25N) (*c*), or GFP::RAB-14(T67M) (*d*). Wild-type RAB-14 and RAB-14(Q70L), which is locked in the GTP-bound state, displayed a punctate staining pattern and surrounded cell corpses (arrows). RAB-14(S25N), a GDP-bound RAB-14, and RAB-14(T67M), the *qx18* mutant RAB-14, lost the punctate staining pattern and did not surround cell corpses (arrowheads). (Scale bars: 10 μm.)

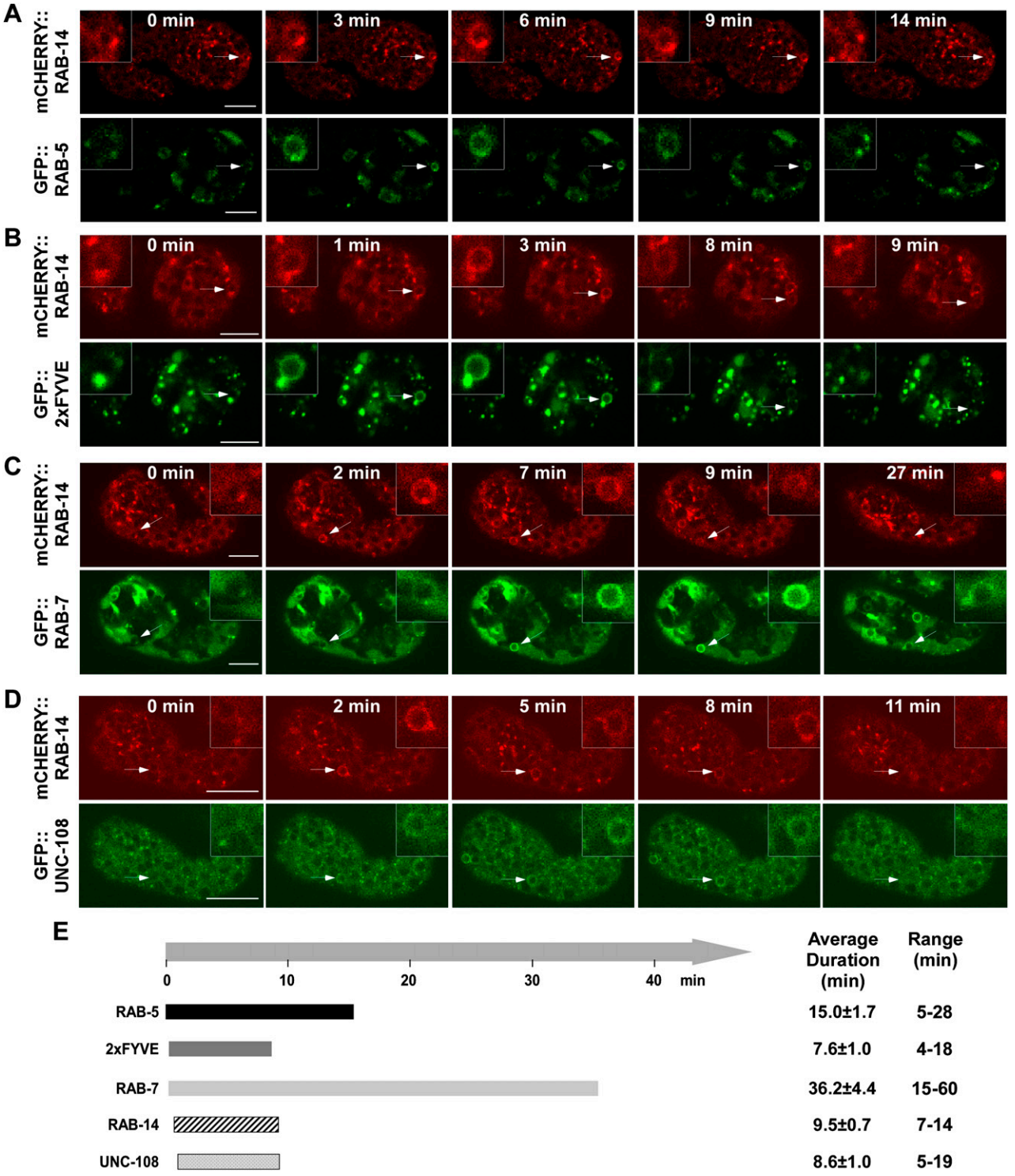

Fig. S4. Recruitment of Rab GTPases to phagosomes in *C. elegans* embryos. Confocol fluorescent time-lapse images of wild-type embryos carrying $P_{rab\text{-}14}$*mcherry::rab-14* in combination with various phagosomal markers: $P_{ced\text{-}1}$*gfp::rab-5* (*A*), $P_{ced\text{-}1}$*gfp::2xFYVE* (*B*), $P_{ced\text{-}1}$*gfp::rab-7* (*C*), and $P_{ced\text{-}1}$*gfp::unc-108* (*D*). Arrows indicate the cell corpses followed. *Insets* show an amplified view of cell corpses with magnification of 3×. (Scale bars: 10 μm.) (*E*) Summary of the temporal order of recruitment of the phagosomal reporters shown in *A–D*. The time point when RAB-5 was detected on phagosomal membranes was set as 0 min. The average duration time (± SEM) and the range of the duration are shown. At least 10 cell corpses were followed. Bars represent mean duration.

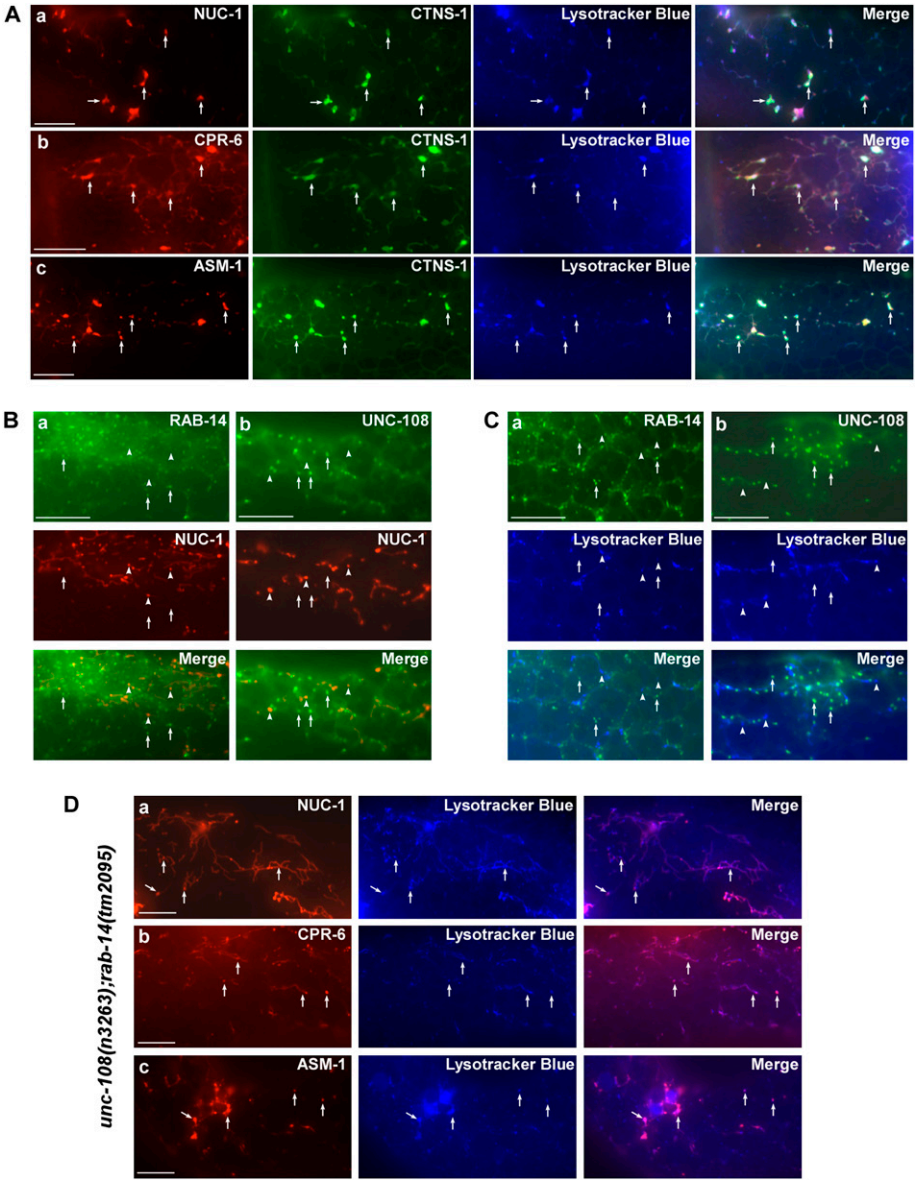

Fig. S5. NUC-1, CPR-6, and ASM-1 localize to lysosomes. (*A*) Fluorescent images of gonadal sheath cells in wild-type animals that carry both $P_{ced\text{-}1}$*ctns-1::gfp* and $P_{ced\text{-}1}$*nuc-1::mcherry* (*a*) or $P_{ced\text{-}1}$*cpr-6::mcherry* (*b*) or $P_{asm\text{-}1}$*asm-1::mcherry* (*c*) and are stained by Lysotracker Blue. NUC-1, CPR-6, and ASM-1 localized to lysosomes as indicated by CTNS-1::GFP and Lysotracker Blue staining (arrows). (*B*) Fluorescent images of gonadal sheath cells in wild-type animals coexpressing $P_{ced\text{-}1}$*nuc-1::mcherry* and P_{hsp}*gfp::rab-14* (*a*), or $P_{ced\text{-}1}$*gfp::unc-108* (*b*). RAB-14- and UNC-108–positive vesicles (arrows) do not overlap with NUC-1–positive puncta (arrowheads). (*C*) Fluorescent images of gonadal sheath cells in wild-type animals that express GFP::RAB-14 (*a*) or GFP::UNC-108 (*b*) and are stained by Lysotracker Blue. RAB-14 and UNC-108 (arrows) did not localize to lysosomes as indicated by positive Lysotracker Blue staining (arrowheads). (*D*) Fluorescent images of gonadal sheath cells in *unc-108(n3263);rab-14(tm2095)* animals that express NUC-1::mCHERRY (*a*), CPR-6::mCHERRY (*b*), or ASM-1::mCHERRY (*c*) and are stained by Lysotracker Blue. The lysosomal localization of above three enzymes (arrows) is not affected in *unc-108(lf);rab-14(lf)* double mutants. (Scale bars: 10 μm.)

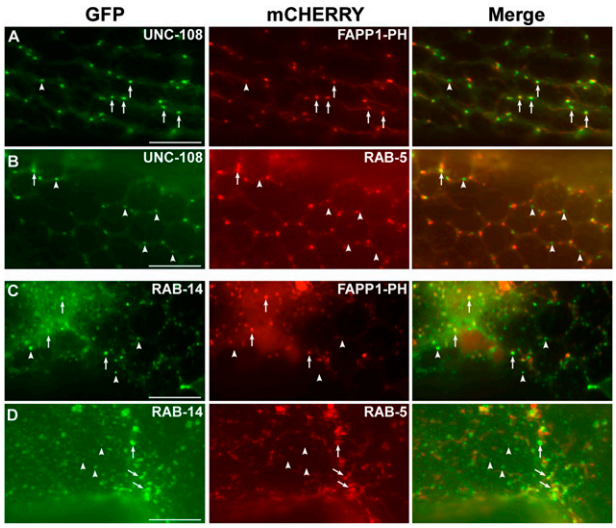

Fig. S6. RAB-14 and UNC-108 localize to early endosomes and the trans-Golgi network in sheath cells. Fluorescent images of gonadal sheath cells in wild type coexpressing GFP::UNC-108 and mCHERRY::FAPP1-PH (*A*), GFP::UNC-108 and mCHERRY::RAB-5 (*B*), GFP::RAB-14 and mCHERRY::FAPP1-PH (*C*), or GFP::RAB-14 and mCHERRY::RAB-5 (*D*). FAPP1-PH specifically labels the trans-Golgi network, whereas RAB-5 localizes to early endosomes. UNC-108 mainly localizes to FAPP1-PH–positive vesicles and very little of it can be seen on RAB-5–positive puncta. RAB-14 shows partial colocalization with both FAPP1-PH and RAB-5. Arrows point to vesicles that are labeled by both UNC-108 (RAB-14) and FAPP1-PH (RAB-5), whereas arrowheads indicate puncta that are stained only by UNC-108 or RAB-14 but not FAPP1-PH or RAB-5. (Scale bars: 10 μm.)

Table S1. Primers used for plasmid construction

Primer	Sequence
PTJH54	GC*GGTACC*ATGACGGCTGCTCCTTAC
PPFG60	GG*GGTACC*CTAGCAGTTGCAGTCCTTCTTC
PTJH48	GC*GCATGC*CCATTCAGGAAGCACGTGAGCGG
PTJH53	GC*GGATCC*TTTTATGTGTTTTTGTTACCTG
PPFG31	TGATATGGGTGTCGGAAAA**AAC**TGTCTTCTTCATCAGTTCAC
PPFG32	GTGAACTGATGAAGAAGACA**GTT**TTTTCCGACACCCATATCA
PPFG53	GATCAAGCTTCAAATCTGGGAC**ATG**GCGGGCCAGGAGCGATTCCG
PPFG54	CGGAATCGCTCCTGGCCCGC**CAT**GTCCCAGATTTGAAGCTTGATC
PPFG33	CAAATCTGGGACACGGCGGGC**CTA**GAGCGATTCCGCGCTGTGAC
PPFG34	GTCACAGCGCGGAATCGCTC**TAG**GCCCGCCGTGTCCCAGATTTG
PTJH48	GC*GCATGC*CCATTCAGGAAGCACGTGAGCGG
PTJH49	GC*GGATCC*GCAGTTGCAGTCCTTCTTCCC
PPFG71	GG*GATATC*CTAGCAGCCACAGCCTTCTCTC
PPFG72	GG*GGTACC*CTAGCAGCCACAGCCTTCTCTC
PPFG285	CGCCC*GGG*ATGGGCTTGTCTCCTGCCGC
PPFG286	GG*GGTACC*TGCACAATTATTTTGGGTTGC
PPFG271	CGCCC*GGG*ATGGTAGGCTTTTGAACTTTG
PPFG272	GG*GGTACC*GTAGTTGTCATCGTAGACGTG
PPFG364	GC*GGTACC*ATGGAGGGGGTGTTGTACAAG
PPFG365	GC*GGTACC*TTAAGTCCTTGTATCAGTCAAAC
PXCW241	GC*GGTACC*ATGGCCGCCCGAAACGCAGGAACC
PXCW243	GC*GGTACC*TTATTTACAGCATGAACCCTTTTG

Restriction sites are italicized; each site has two protective 5′ nucleotides. The sites for introducing point mutations into RAB-14 by in vitro mutagenesis are in bold.